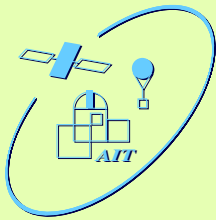


# Survey of Large Planetary Nebulae in Decay

Thomas Rauch, Elise Furlan, Florian Kerber



Institut für Astronomie und Astrophysik, Universität Tübingen, Germany

e-mail rauch@astro.uni-tuebingen.de

Institut für Astrophysik, Universität Innsbruck, Austria

e-mail Elise.Furlan@uibk.ac.at

ST-ECF, Garching, Germany

e-mail fkerber@eso.org



## Abstract

The Planetary Nebulae (PNe) return nuclear processed stellar material into the interstellar medium (ISM) and thus have an important influence on the chemical evolution of our Galaxy. We present results of a survey of PNe in decay which have reached a density comparable to the ambient ISM which leads to an interaction with it. This gives us the opportunity to investigate properties of the ISM. We have identified about 20 new examples for this interaction, demonstrating that it is a more common phenomenon than previously expected. Different stages of interaction, ranging from the early (asymmetric brightness distribution) to the very advanced (parabolic or distorted shape and/or an off-center central star) are obvious.

## Introduction

PNe are the result of heavy mass loss of Asymptotic Giant Branch (AGB) stars. They are successfully explained in terms of the interacting-stellar-winds model by Kwok et al. (1978, ApJ 219, L 125) as the product of the mass-loss history during the stellar AGB and post-AGB evolution.

A somewhat neglected aspect of PNe is that they give evidence for an important process that remains very difficult to study, the return of matter processed within stars to the ISM. This material of course is enriched in heavier elements and leads to the chemical evolution of galaxies.

Old PNe in the process of decay are the very last objects that can be observed before the enriched nebular material is fully dispersed and mixes with the ISM.

## Observation

Over the years interaction of PNe with the ambient ISM has been recognized as a very important process in the late stage of PN evolution. Once considered a curiosity only seen in a few odd examples, like A 35 (Jacoby 1981, ApJ 244, 903; Hollis et al. 1996, ApJ 456, 644) it has now become evident that this process is much more common.

In our ongoing survey we have collected the largest, homogeneous data set on old PNe (Tab. 1) interacting with the ISM, by means of narrow band imaging and long slit spectroscopy. Of the 25 objects studied about 75 % show signs of interaction.

This unexpectedly large percentage may be the result of an observational bias: the interaction leads to an - usually asymmetric - brightness enhancements in these low surface brightness objects facilitating their discovery.

With our new data we are able to identify the full range of phenomena associated with the interaction. This makes it possible to distinguish different stages of interaction, see below. Some examples are shown in Figs. 1, 2, 3, and 4.

## The Interaction Process

A theoretical basis for the understanding of the interaction process has been laid by Borkowski et al. (1990, ApJ 360, 173) and Soker et al. (1991, AJ 102, 1381). When the PNe are moving with respect to the ISM, we can distinguish different stages of interaction:

- young PNe
  - density of PN  $\gg$  density of ISM
  - free expansion of PN
  - no significant influence of ISM
- mid-age PNe
  - density of PN decreases
  - ISM pressure upstream  $\approx$  pressure in PN shell
  - PN shell is compressed
  - increase of PN density and surface brightness, asymmetric brightness distribution
  - higher recombination rate → lower degree of ionization
  - Mach number still large → shape of PN not significantly affected, largely spherical
- old PNe
  - PN density drops further
  - expansion is slowed upstream → deformation of PN (blunt parabola)
  - Rayleigh-Taylor instabilities lead to severely distorted PN shape
  - central star moves out of the PN center

Name	PN	$\alpha_{2000}$	$\delta_{2000}$	$\varnothing''$
KLW 11	G 193.0	-04.5 05 <sup>h</sup> 57 <sup>m</sup> 08 <sup>s</sup>	+15° 25' 31"	70 × 80
KLW 12	G 197.0	+05.0 06 <sup>h</sup> 43 <sup>m</sup> 26 <sup>s</sup>	+16° 48' 53"	31 × 35
EGB 9	G 209.4	+09.4 07 <sup>h</sup> 19 <sup>m</sup> 01 <sup>s</sup>	+07° 23' 17"	377 × 234
KeWe 3	G 238.4	-01.8 07 <sup>h</sup> 33 <sup>m</sup> 25 <sup>s</sup>	-23° 25' 44"	283 × 306
MeWe 1-1	G 272.4	-05.9 08 <sup>h</sup> 53 <sup>m</sup> 37 <sup>s</sup>	-54° 05' 08"	143 × 165
NeVe 3-1	G 275.9	-01.0 09 <sup>h</sup> 34 <sup>m</sup> 01 <sup>s</sup>	-53° 11' 89"	62 × 53
Lo 4	G 274.3	+09.1 10 <sup>h</sup> 05 <sup>m</sup> 46 <sup>s</sup>	-44° 21' 33"	55 × 68
MeWe 1-2	G 283.4	-01.4 10 <sup>h</sup> 14 <sup>m</sup> 24 <sup>s</sup>	-58° 11' 49"	272 × 265
NeVe 3-6	G 292.5	+00.9 11 <sup>h</sup> 25 <sup>m</sup> 43 <sup>s</sup>	-60° 14' 30"	38 × 58
KFR 1	G 296.3	+03.1 12 <sup>h</sup> 00 <sup>m</sup> 15 <sup>s</sup>	-59° 04' 34"	90 × 100
HaTr 1	G 299.4	-04.1 12 <sup>h</sup> 16 <sup>m</sup> 33 <sup>s</sup>	-66° 45' 46"	76 × 73
WeKG 2	G 308.4	+00.4 13 <sup>h</sup> 38 <sup>m</sup> 42 <sup>s</sup>	-61° 55' 45"	42 × 35
SuWt 1	G 309.2	+01.3 13 <sup>h</sup> 43 <sup>m</sup> 59 <sup>s</sup>	-60° 49' 42"	94 × 53
MeWe 2-4	G 314.0	+10.6 14 <sup>h</sup> 01 <sup>m</sup> 15 <sup>s</sup>	-50° 40' 12"	480 × 400
MeWe 1-4	G 315.9	+08.2 14 <sup>h</sup> 17 <sup>m</sup> 30 <sup>s</sup>	-52° 26' 19"	113 × 148
LoTr 10	G 316.3	-01.3 14 <sup>h</sup> 46 <sup>m</sup> 20 <sup>s</sup>	-61° 13' 30"	56 × 45
Lo 10	G 320.2	+01.3 15 <sup>h</sup> 49 <sup>m</sup> 29 <sup>s</sup>	-52° 30' 17"	31 × 31
K 1-31	G 335.4	+09.2 15 <sup>h</sup> 53 <sup>m</sup> 13 <sup>s</sup>	-41° 50' 25"	34 × 32
HaTr 3	G 333.4	-04.0 16 <sup>h</sup> 39 <sup>m</sup> 38 <sup>s</sup>	-52° 49' 11"	43 × 43
KeWe 5	G 348.9	+04.6 16 <sup>h</sup> 57 <sup>m</sup> 56 <sup>s</sup>	-35° 24' 56"	20 × 17
Tc 1	G 345.2	-06.8 17 <sup>h</sup> 45 <sup>m</sup> 35 <sup>s</sup>	-46° 05' 23"	57 × 57

Table 1. Summary of the analyzed PNe in our survey. MeWe 1-1, KFR 1, SuWt 1, and MeWe 1-4 are shown in Figs. 1, 4, 2, and 3, respectively

## Acknowledgements

This research was supported by the DARA/DLR under grants 50 OR 9409 1 and 50 OR 9705 5 (TR), and in part by the "Auslandsabteilung" of the University Innsbruck (EF).

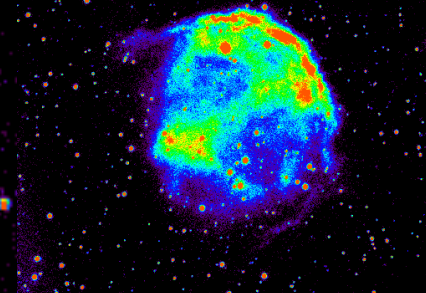


Fig. 1. MeWe 1-1. [N II] image (3.8' × 3.8', 600 sec) taken at LCO in Feb. 1998

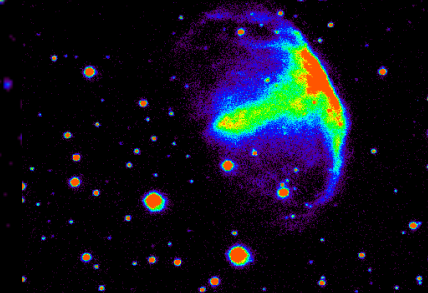


Fig. 2. SuWt 1 — The Hammer Nebula. H alpha image (1' × 1', 600 sec) taken at LCO in Feb. 1998

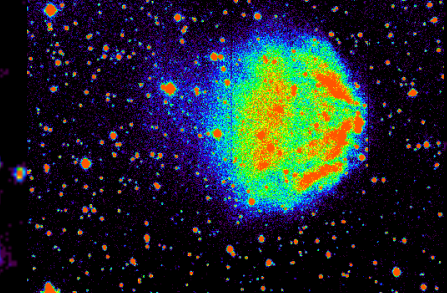


Fig. 3. MeWe 1-4. H alpha + [N II] image (3.9' × 3.9', 1 800 sec) taken at LCO in Feb. 1998

Fig. 4. KFR 1 — The Jelly-Fish nebula. H alpha image (5.5' × 5.5', 900 sec) taken at the 100" "du Pont" telescope at Las Campanas Observatory (LCO) in Feb. 1998